MRS Communications (2015), *5*, 423–434
doi:10.1557/mrc.2015.56

MRS Communications

Polymers/Soft Matter Prospective Article

Polymer films of nanoscale thickness: linear chain and star-shaped macromolecular architectures

Peter F. Green*, Department of Materials Science and Engineering, Department of Chemical Engineering, Biointerfaces Institute, University of Michigan, Ann Arbor, Michigan 48109, USA
Emmanouil Glynos, Institute of Electronic Structure and Laser, Foundation for Research and Technology—Hellas, P.O. Box 1385, Heraklion, Crete GR 71110, Greece
Bradley Frieberg, Materials Science and Engineering Division, National Institute of Standards and Technology, Gaithersburg, Maryland 20899, USA
Address all correspondence to Peter F. Green at **pfgreen@umich.edu**

(Received 23 April 2015; accepted 15 July 2015)

Abstract

Applications of polymer thin films include functional coatings, flexible electronics, membranes and energy conversion. The physical properties of polymer films of nanoscale thicknesses typically differ from the bulk, due largely to entropic effects and to enthalpic interactions between the macromolecules and the external interfaces. Studies of the size-dependent physical properties of macromolecules have largely been devoted to linear chain polymers. In this Prospective, we review recent experiments and simulations that describe the structure and fascinating physical properties, from wetting to the glass transition, of star-shaped macromolecules. The properties of these molecules would render them more useful than their linear chain analogs, for some specific applications.

Introduction

Molecular design strategies have enabled the synthesis of polymers with functionalities that render them useful for diverse thin-film applications. Notable examples include organic solar cells, thermoelectrics, organic light-emitting diodes, energy storage devices, as well as active and passive coatings. The materials used in these applications include homopolymers, copolymers, polymer/polymer mixtures, and polymer nanocomposites (nanoparticles of varying functionalities incorporated within polymer hosts). While the possibilities for literally "tailoring" the functional properties of polymeric materials through the processing of different combinations of polymers, and in some cases nanoparticles, appear to be virtually limitless, the technical challenges are important. Collective entropic and enthalpic interactions over varying length-scales lead to unusual and often complicated morphological structures. Moreover, long-term reliability issues often pose additional difficulties for some applications. In general, understanding and optimizing the synthesis–processing–property–function–reliability of polymer-based material systems, while offering enormous technological opportunities, pose important scientific challenges.

An important goal of this Prospective is to describe the manner in which physical properties of polymers confined to nanoscale thickness dimensions differ from the bulk.[1–7] Examples of thickness dependent physical properties of polymers include the following. Perhaps one of the best-known example of this phenomenon is the thickness, h, dependence of the average glass-transition temperature, T_g, of a sufficiently thin homopolymer film, as revealed by experiment, theory, and simulations.[1–3,6–12] The thickness dependence of T_g is exhibited by thin films typically in the thickness range of nanometers to tens of nanometers, stemming from interfacial effects. Other examples of thickness-dependent properties include the mechanical properties of thin polymer films,[13,14] gas permeation in thin films,[15,16] and the mobility of charge carriers in polymers.[17–19] The h-dependencies of these properties typically occur over much longer length-scales, in some cases a few hundred nanometers, than those of the glass transition. In the case of polymer-A/polymer-B mixtures, in contrast to metallic alloys and small molecule mixtures, phase separation temperatures may differ from the bulk by tens of degrees and the length-scales may be as long as hundreds of nanometers.[20–24] This is in part due to entropic effects, associated with the fact that the A and B constituents are long chains; each chain is composed of hundreds or thousands of monomers connected by covalent bonds. For the final example, we note that shifts of phase separation temperatures (i.e., so-called order–disorder transitions) are also documented for diblock copolymer thin films supported by substrates.[25–27] Therefore the length-scales over which this h-dependent phenomenon occurs depend on the specific property, the polymer, and on the polymer/external interface system.

* This author was an editor of this journal during the review and decision stage. For the MRC policy on review and publication of manuscripts authored by editors, please refer to http://www.mrs.org/editor-manuscripts/.

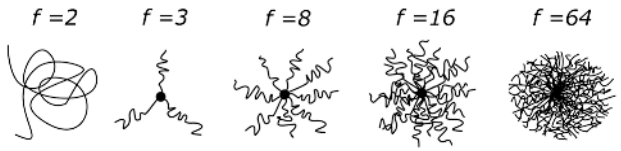

Figure 1. The architectures of a linear chain and of the star-shaped macromolecules of different functionalities (number of arms per molecule) are shown here. The number of monomers per arm is N_{arm}. ($N_{arm} = M_{arm}/M_0$, where M_0 is the molecular weight per monomer, and M_{arm} is the molecular weight per arm.)

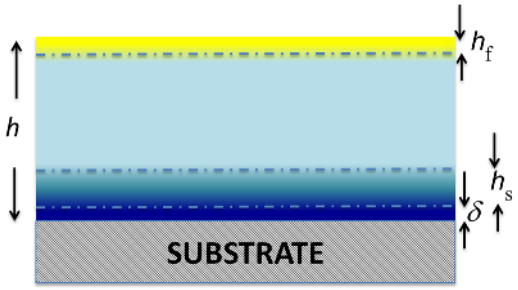

Figure 2. Schematic illustrates variations in the local density of the segmental "packing" at distances away from the interfaces.

Much of what we understand about the effects of film thickness confinement on the physical properties of polymers is based on studies of linear chain macromolecules, comparatively little is understood about confinement effects the physical properties of macromolecules of different architectures, such as star-shaped macromolecules. It has been demonstrated that for star-shaped polymers the physical properties, such as wetting,[28,29] thin-film glass-transition temperatures,[30,31] and physical aging,[32,33] differ appreciably from those of linear chain polymers. Wang et al. have demonstrated, using x-ray photon correlation spectroscopy, that in contrast to linear-chain thin-film polymers the surface viscosities of branched macromolecules are larger than the bulk.[34,35] Other studies provide more general insights into how changes in the structure of star-shaped polymers, achieved by varying the functionality, f (number of arms per molecule), and the molecular mass per arm M_{arm} (see Fig. 1), may influence certain physical properties, such as the bulk rheological behavior.[36–38]

This Prospective discusses fundamental questions related to the structure–property behavior and potential applications of star-shaped polymer films in the nanoscale thickness range. Our discussion will focus on differences between the structures of linear-chain and star-shaped macromolecular thin films and related implications for three important physical properties: glass transition, wetting, and physical aging.

Effect of geometric confinement on the structure of polymers

The adsorption of a polymer chain onto a surface is driven by the competition between enthalpic and entropic interactions: the gain in enthalpy due to the binding of monomers from the chain onto the surface and the associated conformational entropic cost associated with this adsorption.[39,40] As a result, the "packing" of segments of chains is not spatially uniform throughout a polymer film. At a hard, atomically smooth substrate, the average monomer density is higher than in the bulk; simulations reveal that the amplitude of the monomer density profile oscillates away from the substrate, with the amplitude decreasing gradually into its bulk value.[41–44] Such simulations further suggest a "layering" of the segments at the substrate, including the center of mass of the chain. Specifically, the component of the radius of gyration of a chain parallel to the wall, $\langle R_{xy} \rangle$, is larger than $\langle R_z \rangle$, that of the radius of gyration component normal to the wall.

At an unconstrained or free surface, simulations of linear-chain polymers reveal that the local segmental "packing" is lower than the bulk.[44–46] Experimental studies using positron annihilation lifetime spectroscopy (PALS) reveal the presence of increased free volume at the free surface in relation to the bulk.[30,31] This is experimental evidence that supports the premise that the chain segments near a free surface possess larger configurational freedom than the bulk. Simulations also show that the sharpness, or breadth, of this interface increases with decreasing temperature.[44–46] In typical polymer systems, the length scales of the breadth of such an interface are of the order of nanometers. To this end, we schematically illustrate in Fig. 2 the local packing density of a supported polymer film, confined between a free surface and a hard interface. In this figure, the overall film thickness is h; h_f is the length-scale from the free surface where there would be increased configurational freedom. The length-scale δ, of the order of a nanometer, is the thickness from the substrate where the chain segment orientations are restricted and there is a preferential orientation of the segments in the plane of the film. The distance $h_s + \delta$ is the length-scale (~ few nanometers) over which the density of the film is perturbed due to the substrate. In addition to changes in the density at an interface, the average molecular weight between entanglements near an interface differs from the bulk and this can have important implications on mechanical properties, including interfacial adhesion and fracture.[47] Other physical properties, such as the time-dependent displacements of chain segments in thin films, would differ from the bulk[48–50]

Generally polymer segmental dynamics at polymer/substrate interfaces are comparatively slow;[50–53] this sluggishness is believed to be due to the long time-scales (compared with bulk relaxations) associated with adsorption/desorption of segments from the "walls."[54] Stronger interactions with the walls lead to longer desorption times, thereby leaving the molecules in a metastable state, and hence slower dynamics. In fact, broad band dielectric spectroscopy (BDS) studies reveal a reduction of the dielectric strength ($\Delta\varepsilon$) indicating a portion of the film is "dead" when the chains are permanently adsorbed onto a

substrate and the dipoles unable to reorient.[52] This effect, permanently adsorbed chain segments, is polymer/substrate specific and typically occurs after heating the film for sufficiently long periods of time. Simulations reveal that the dynamics at "walls" are anisotropic; the dynamics of the segments normal and parallel to the substrate differ in magnitude.[55,56]

With regard to free, unconstrained, surfaces it has been demonstrated by experiments and by simulations that the polymer chain dynamics are fast relative to the bulk.[1–10,57–64] The dynamics near the free surface are enhanced due to excess configurational freedom of the chain segments. The excess configurational freedom would be responsible for a reduction of the effective friction coefficients, which dictate the time scales of the center-of-mass diffusion of chains near a surface, leading to an increase in translational diffusion coefficient of a chain.[65] Later it will be shown that changes in physical properties of polymers occur over much longer length-scales than the length scales that characterize changes in their segmental densities at interfaces.

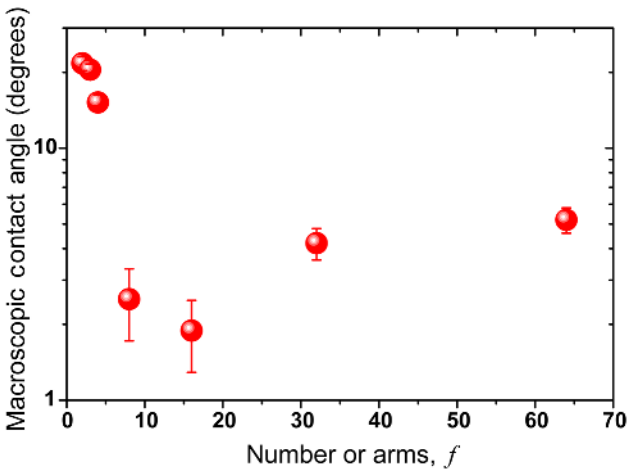

Figure 3. Equilibrium contact angles, θ_{eq}, are plotted as a function of f. Reproduced (adapted) with permission from Ref. 28, copyright 2014 American Chemical Society.

Wetting of star-shaped macromolecules

Differences between the wetting properties of star-shaped macromolecules and their linear-chain analogs are profound. To understand these differences it is instructive to recall basic ideas about the wetting of a non-volatile liquid droplet on a substrate.[66–70] The wetting of a liquid on a substrate is dictated by a combination of short- and long-range intermolecular forces: within a specific distance of the line of contact the shape of the droplet is distorted by the intermolecular forces. The molecular length associated with the long-range van der Waals interactions is defined as:

$$\alpha = \sqrt{-A/G\pi\gamma}, \tag{1}$$

where A is the Hamaker constant, and γ the liquid/vapor surface tension of the liquid. The macroscopic angle of contact θ_{eq}, defined away from the line of contact, is dictated by Young's equation, which relates it with interfacial energies:

$$\gamma\cos\theta_{eq} = \gamma_{SV} - \gamma_{SL}, \tag{2}$$

where γ_{SV} is the surface tension, and γ_{SL} is the interfacial tension between the liquid and the substrate.

Recently we showed that the macroscopic contact angle θ_{eq} for an 8-arm star-shaped polystyrene (PS) macromolecule on silicon oxide substrates (SiO_x) is approximately one order of magnitude smaller than linear-chain PS on the same substrate.[28,29] The adsorption of a macromolecular segment onto a substrate is largely dictated by a competition between the gain of enthalpy due to binding monomers to the substrate, and the conformational entropic cost of adsorption. The enhanced wetting of the star-shaped macromolecules is associated with the fact that these branched polymeric molecules experience smaller losses in configurational entropy when adsorbed to interfaces compared with their linear analogs.[71–75] These smaller losses of configurational entropy of the star-shaped macromolecules, in relation to their linear chain analogs of the same total number of monomers, may be considered to be an entropic attraction of the star-shaped molecules to the substrate.

The data in Fig. 3 describe the fascinating wetting characteristics of the star-shaped macromolecules.[28] The error bars this figure represent were determined from measurements of the contact angles of tens of droplets. It is shown that the macroscopic contact angle rapidly decreases with increasing functionality of the star, before exhibiting a minimum at $f = 16$. For $f > 16$, θ_{eq} increases with f until it becomes nearly constant in the high functionality limit. The values are smaller than that of linear chains.

The wetting behavior of star-shaped molecules in relation to their linear-chain analogs may not be fully understood in terms of the surface tension of the molecules; effects associated with the entropic attraction must be considered. The surface tension for star-shaped polymers is reasonably well described by:

$$\gamma^s(M_n) = \gamma^s(\infty) + \rho RT\frac{fU^e + U^b}{M_n^s}, \tag{3}$$

where $\gamma(\infty)$ is the surface tension of the theoretical infinite number average molecular mass polymer, ρ is the bulk density, R is the universal gas constant, T is the temperature, M_n is the number average molecular mass, and U^e and U^b represent the effective attractive, or repulsive, interactions between the interface and the chain ends, and branch points, respectively.[72,73] Because this relationship predicts a monotonic decrease of the surface tension with increasing functionality, the non-monotonic behavior of θ_{eq} cannot be explained solely in terms of changes in the surface tension. As discussed below, the wetting properties of star-shaped polymers stem primarily

from the strong surface adsorption behavior in relation to linear chains of otherwise identical chemical structure.

Molecular dynamics (MD) simulations of a bead-spring model of polymer chains show that the ratio of the perpendicular and parallel components of the radii of gyration, $\langle R_g^2\rangle_z/\langle R_g^2\rangle_{xy}$, of macromolecules adsorbed to an interface depends on the functionality of the polymer [Fig. 4(a)].[28] These MD simulations indicate that $\langle R_g^2\rangle_z/\langle R_g^2\rangle_{xy}$ increases with increasing f, but exhibits a maximum for $f \approx 8$. Beyond this maximum, $f > 8$, the ratio decreases and reaches a constant value in the high f limit. The densities of adsorbed chains, ρ_{ads} (the number of adsorbed chains per unit area), extracted from the MD simulations and experimental measurements are plotted in Fig. 4(b). These data indicate that dependence of ρ_{ads} on f is consistent with the $\langle R_g^2\rangle_z/\langle R_g^2\rangle_{xy}$ [Fig. 4(a)] versus f trends.

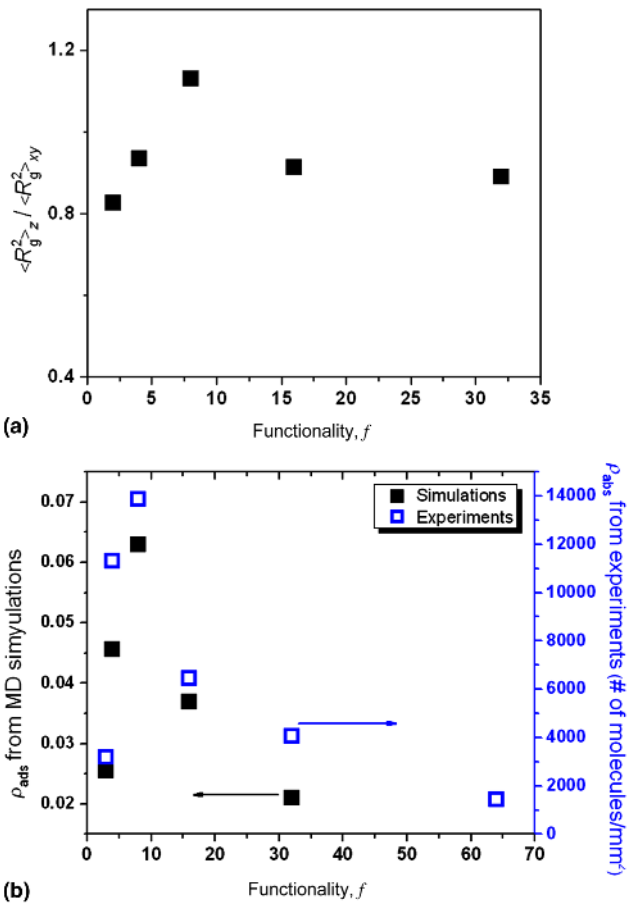

Figure 4. (a) The ratio of the parallel and perpendicular components of the mean-square radii of gyration $\langle R_g^2\rangle_z/\langle R_g^2\rangle_{xy}$ of the adsorbed polymers is plotted as a function of f. Reproduced (adapted) with permission from Ref. 28, copyright 2014 American Chemical Society. (b) The number of adsorbed chains per unit area (density), ρ_{ads}, is shown as a function of f, obtained from the experiment and from the simulations. Reproduced (adapted) with permission from Ref. 28, copyright 2014 American Chemical Society.

The maxima of the anisotropy of orientation of the molecules and of the density [data in Figs. 4(a) and 4(b)] are due to the same two competing mechanisms. The entropic attraction of a star-shaped molecule to the substrate increases as the functionality f of the molecule increases. Additionally with this increase of f, entropic intermolecular repulsions between the arms of a molecule extending from the branch point necessarily increases; this leads to stretching of the arms (i.e., a reduction of the entropy per chain). This intermolecular repulsion has the effect of reducing any potential "crowding" of the molecules at a surface. In other words, the entropic restrictions imposed by increasing f lead to a decreasing compliance of the star-shaped polymers, which suppresses their ability to deform on the surface when adsorbed. Hence, the angle of contact decreases.

This is the first time that such significant differences in the wetting behavior are achieved by simply changing the architecture of the molecule, without changing the chemistry. The practical implications are that the wetting at an interface may be "tailored" via changes in the functionality and the length of the arms of the macromolecule.

Glass transition of thin films

This topic is introduced by recalling that the reduction of the temperature of substances, from small molecule liquids to network glass melts and polymer melts, is accompanied by a significant increase in the structural relaxation time. Practically, at a sufficiently low temperature where the structural relaxation time becomes longer than the observation time, or duration, that the cooling rate permits, the system becomes "frozen," this temperature denotes the glass transition. Additionally virtually any substance, if cooled at a sufficiently rapid rate, would not crystallize due to a lack of time for the constituents to form an ordered structure. It is important to note that by virtue of their molecular structures, atactic polymers for example, will not crystallize and therefore exhibits a T_g, regardless of cooling rate. Glass-forming melts solidify, with the absence the formation of long-range order, at a lower temperature than the crystallization temperature. The glass-transition temperature, T_g, occurs over a very narrow range of temperatures and is cooling-rate dependent. With these brief comments, we discuss this phenomenon with regard to the behavior of thin polymer films.

It is a known fact that the average glass-transition temperature of a sufficiently thin polymer film differs from the bulk.[8,63,76–79] This effect is often observed when the polymer film is of the order of tens of nanometers, whether or not it is supported by a substrate. In the case of freely standing linear-chain polymer films, the average T_g decreases with decreasing h. When the polymer films are supported by non-wetting surfaces, such as linear-chain PS supported by SiO_x, the average T_g decreases with decreasing h (see Fig. 5).[2,80] However, when the interactions between the polymer and the substrate are sufficiently strong (i.e., polar interactions), the average T_g increases with decreasing h. Two examples of this are poly(methyl methacrylate) (PMMA) films supported by SiO_x

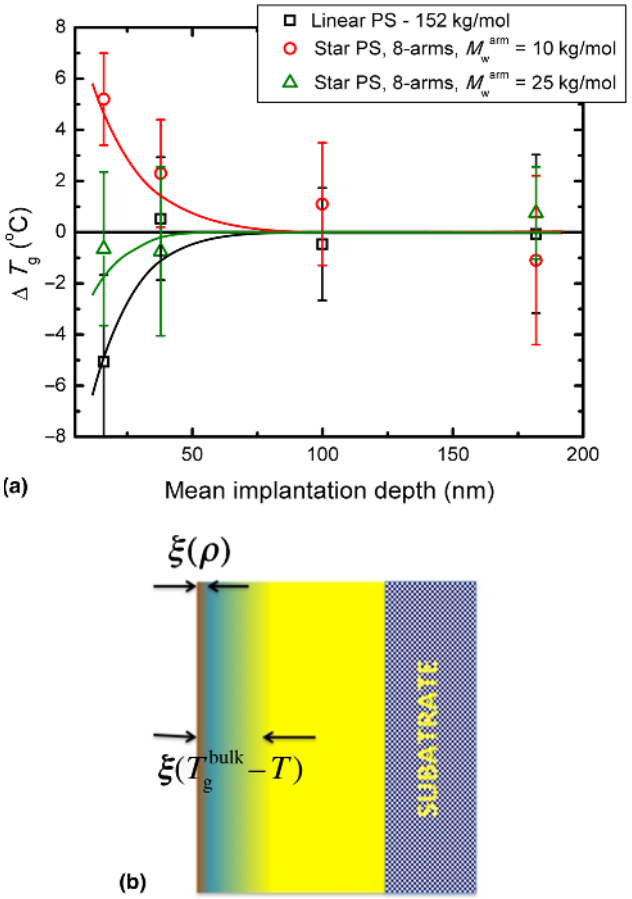

Figure 5. (a) T_g, plotted as a function of depth, for linear-chain PS and for star-shaped PS ($f = 8$, $M_{arm} = 10$ and 25 kg/mol.); these data were obtained using depth-profile PALS. Reproduced (adapted) with permission from Ref. 32, copyright 2012 American Physical Society and Ref. 30, copyright 2011 American Physical Society. (b) The relative length scales of the effects of the monomer density profiles and of the T_g are depicted here.

and PS supported by gold substrates.[1,81–84] The important point is that the average glass-transition temperature of a thin polymer film is influenced by the polymer and by the nature of the interactions between the polymer segments and the external interfaces, as further discussed below.

It has been suggested that due to the lower segmental configurational freedom of chains at a free surface, the T_g at the free surface would be lower than the bulk.[58] Experiments show that polymer segments, within a distance of a few nanometers of the free surface, remain mobile at temperatures below the bulk T_g.[57,59–62,85] Commensurate with this observation, depth-profile PALS measurements demonstrate that the glass-transition temperature at the free surface of linear polystyrene is lower than the bulk; these data are shown in Fig. 5(a) (squares).[30,32] The T_g becomes equal to the bulk at a distance of tens of nanometers into the film. Other experiments also lead to conclusions that the T_g across the film is not uniform.[4,60] For the case of PS/SiO_x where the interactions between the PS chain segments and SiO_x are non-wetting, and the T_g at the free surface is lower than the bulk, the average T_gs of such PS films are lower than the bulk value. Generally, when the T_g at the free surface is lower than the bulk and the polymer/substrate interactions are sufficiently weak, the average T_{gS} of sufficiently thin polymer films are lower than the bulk. However, if the polymer substrate interactions are sufficiently strong (e.g., hydrogen bonding), and responsible for an enhancement of the local T_g at the substrate, then the average T_g of a sufficiently thin film may be larger than the bulk value. The PS/Au and PMMA/SiO_x systems are excellent examples.

It is important to recognize that the length-scale ξ_ρ over which the "packing" of segments is influenced by the proximity to the interface is of the order of a nanometer.[8,64,86] However, the length-scale ξ_{glass} over which the glass-transition temperature deviates from the bulk is at least one order of magnitude larger (Fig. 5). This behavior has not been fully captured using simulations. However, a recent analytical theory provided the first explanation for the differences between the length-scales associated with segmental packing and those longer distances associated with changes in the glass transition.[87] The displacements of polymer segments are associated with long-range collective elastic distortion processes, occurring over tens of nanometers. Near a surface the effects are different from the bulk due to the "reduced neighbors" and subtle differences in the "packing" of segments. For this reason, the near surface and the bulk vitrification temperatures, and their associated length scales, are different.

Since the star-shaped macromolecules experience lower entropic penalties than their linear-chain analogs when adsorbed at an interface, it would be reasonable that their thin-film glass-transition temperatures would differ from linear chains, as suggested by the data in Fig. 5(a).[28,29,71–75] To this end the h-dependencies of the average T_gs of several different star-shaped PS thin films supported by SiO_x substrates are reported in Fig. 6. In this figure, M_{arm} was fixed and the functionalities are varied, $3 < f < 64$. For cases where $f = 2$, 3, and 4 the average T_gs decrease with decreasing h. This behavior is similar to linear-chain PS, where T_g decreases with decreasing h.[30] However, for molecules possessing functionalities in the range $4 < f < 32$, the average T_gs increase with decreasing h. This remarkable shift in the trend, based on the functionality, exhibited by vitrification of the films is more clearly illustrated in Fig. 6(b). In this figure, the T_gs of different $h = 30$ nm thick films of molecules of varying f relative to the bulk T_gs are plotted. It is apparent that the T_g behavior of the star-shaped polymers is similar to that of linear chains when the arms are sufficiently long (M_{arm} is sufficiently high); here the effect of the functionality is not important.[30] Simulations reveal an enhancement of the segmental densities of short-arm star-shaped molecules at the external interfaces, in relation to the bulk. The enhancement at the free interface is less pronounced than at the substrate, which is not unexpected. These results provide a rationale for the shifting trends of the T_g versus h behavior.

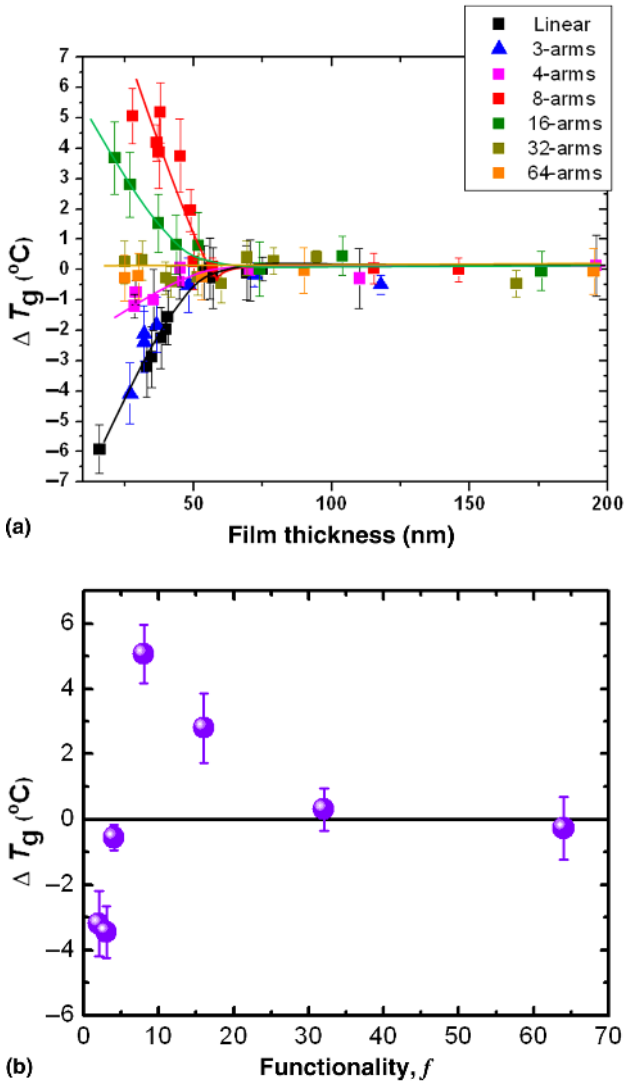

Figure 6. (a)The glass-transition temperatures are plotted as a function of film thickness for linear-chain PS, supported by SiO_x, and for star-shaped PS molecules of varying functionalities. The molecular mass per arm of each macromolecule is ≈10 kg/mol. Reproduced (adapted) with permission, from Ref. 31, copyright 2015 American Chemical Society, and Ref. 30, copyright 2011 American Physical Society. (b) The deviation of T_g from the bulk for a h = 30 nm thick PS film on SiO_x as a function of the number of arms. Reproduced with permission (Ref. 31), copyright 2015 American Chemical Society.

We now discuss the increase of the T_g with decreasing h, for $f > 4$. PALS measurements show that the free surface T_g for the 8-arm star-shaped films is higher than the bulk (Fig. 5). Our MD simulations reveal that at the free surface, the packing density of the 8-arm star-shaped macromolecules is higher than the bulk. Additionally, a strong positional correlation between the star-shaped molecules (spatial ordering of the cores) near the free surface occurs.[31] As described in the previous section, the star-shaped molecules in this regime exhibit a stronger tendency to adsorb to the substrate. This results in a higher packing density and thus a larger local T_g at the substrate interface.

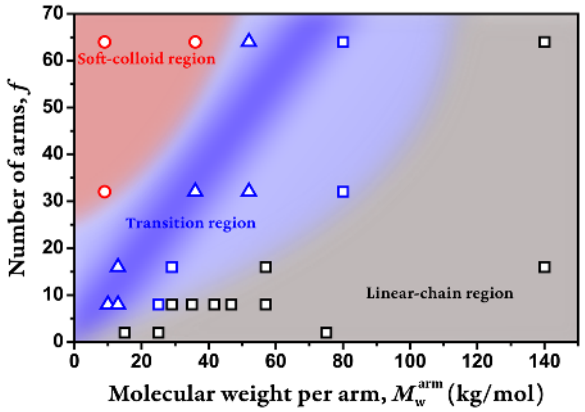

Figure 7. The relative glass-transition temperature, $\Delta T_g = T_g(h = 30\ \text{nm}) - T_g$ (bulk), is shown here for star-shaped polymers of varying functionalities and arm lengths. Gray region (black squares) represents $\Delta T_g < 0$, blue region (blue triangles) represents $\Delta T_g > 0$, and the red region (red circles) represents $\Delta T_g = 0$. Reproduced with permission from Ref. 31, copyright 2015 American Chemical Society.

Because the T_gs at the free surface and at the substrate are larger than the bulk for the 8-arm star with $M_{arm} = 10$ kg/mol., the average T_g of this system increases with the decreasing film thickness [Fig. 6(a)].[30] When arms are sufficiently long, $M_{arm} > 25$ kg/mol., the thickness-dependent T_g behavior is virtually identical to that of linear-chain PS. These results confirm the notion that the thickness dependence of the T_g may be understood in terms of the interactions between the polymer segments with its external interfaces. The interactions are enhanced due to the entropic attraction of the chains to the interfaces with increasing f. As described in the previous section this enhanced entropic attraction is offset by an entropic effect associated with crowding, and an associated loss of mechanical compliance, of the molecules as f further increases. This behavior is largely responsible for the maximum in Fig. 6.

The glass transition of star-shaped PS polymer films on SiO_x may be summarized in terms of a "Diagram of States" where the deviation of T_g from the bulk is illustrated as a function of f and M_{arm} in Fig. 7. When the number of arms is sufficiently large and the arms are sufficiently short, the star-shaped molecules "pack" like soft-colloids; the average glass transition temperatures of these films are equal to that of the bulk. It has also been reported in that bulk star-shaped molecules with high f and low M_{arm} exhibit behavior akin to that of soft-colloids.[36–38] In this regime the molecules self-assemble to form ordered structures and uniform ordered layers across the film. This is illustrated in Fig. 8 with an atomic force microscopy (AFM) image, line-scan and schematic. This organization is consistent with the simulations, which suggest evidence of ordering of the cores of the molecules at the interfaces, for the molecules with large f.

The decreased compressibility of the polymers, with increasing f and decreasing M_{arm} would have the effect of suppressing the influence of the interface on wetting and

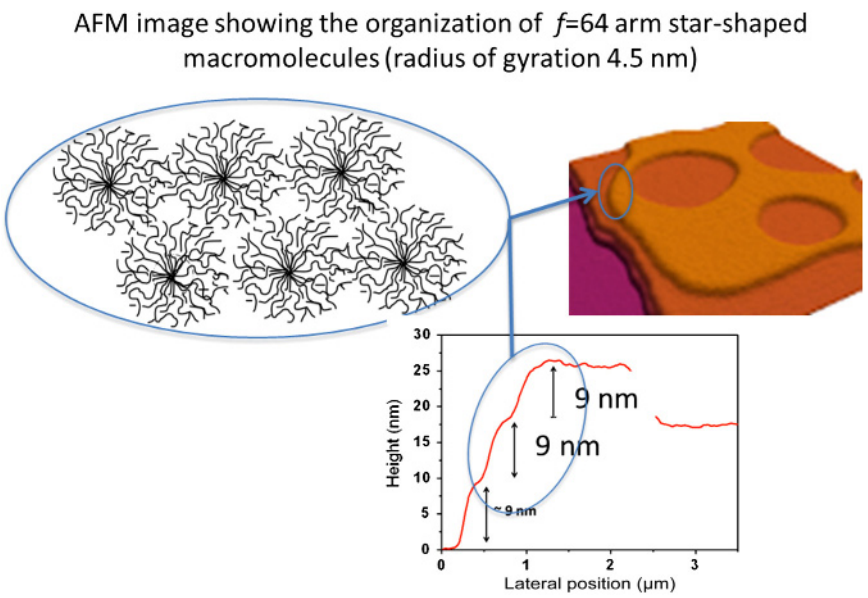

Figure 8. An AFM image of a thin-film star-shaped macromolecule of functionality $f = 64$ (and $M_{arm} \sim 9$ kg/mol.) is shown. The thickness of each layer is represented by the line scan; a schematic representation of the organization of two layers of molecules is shown.

adsorption, and therefore changes in the glass transition as shown. In the "linear-chain" region of Fig. 7, the average T_g of thin films is lower than the bulk. The transition between the linear-chain region and the soft colloidal-like behavior occurs over limited values of f and $M_{arm.}$ This is this region that represents the maximum in Fig. 6(b).

The primary message of this section is that the average T_g of a thin polymer film is dependent on the thickness of the film, the macromolecular architecture and the external interfaces. These data in Fig. 7 illustrate the fact that the glass-transition temperatures of films may be "tailored" simply by changing the macromolecular architecture. The glass-transition temperature is not constant throughout the film; it is a function of the proximity to an interface. Secondly, the architecture of the molecule and the interactions between the molecule and the interfaces have a significant impact on the magnitude of the local T_g and hence the average T_g of the film. The primary implication of these results is that when a thin film is cooled to lower temperatures, different regions within the thin film, based on their proximities to the interfaces, fall out of equilibrium at different temperatures. This has important implications on processing and on properties such as physical aging, which we discuss in the next section.

Physical aging of thin films

The term physical aging refers to a system undergoing slow dynamics as the system approaches equilibrium, due to frustration associated with transitions between the metastable states (configurations).[88] This phenomenon is ubiquitous, occurring in diverse systems: network glasses (i.e., SiO_2),[89] spin glasses,[90] colloids,[90] metallic glass,[91] and polymer glasses.[88]

To understand this phenomenon in polymers we begin by recalling that as the temperature of a glass-forming liquid is decreased, the structural relaxation time, and the viscosity, increases in a non-linear manner. The temperature dependence of the viscosity is well described by the Vogel–Fulcher–Tammann (VFT)[92–94] equation [also equivalently the Williams–Landel–Ferry equation (WLF)]:[95]

$$\eta(T) = Aexp\left(\frac{B}{T - T_\infty}\right), \quad (4)$$

where T_∞ is the Vogel temperature, which is related to T_g, and B is a parameter associated with thermally activated processes. Adam and Gibbs, in 1965, were the first to propose the existence of cooperativity between the dynamics of the constituents of the material and the effect of cooperativity on the overall dynamics. Specifically, there exists a length-scale, ξ_{coop}, which characterizes a distance over which the dynamics are highly cooperative. They, and now others, argue that it is the increase of ξ_{coop} with decreasing T that is responsible for the increase in the activation energy and hence the non-linear increase of time scales of the relaxation dynamics, with decreasing T.[96]

It is currently understood that the dynamics of liquids are spatially and temporally heterogeneous.[97] Specifically, the dynamics of local regions (size $\sim$ nm at high T) vary spatially; in some local regions the dynamics are very fast compared with the average and for others the dynamics are slow compared with the average. The positions of these local regions are correlated temporally in space over particular length-scales ξ_{het} of the order of nanometers.[10,96–99] It is suggested by dynamic heterogeneity models that density fluctuations throughout the

system are responsible for the strong spatial variations of the dynamics. It is the percolation of the slow domains that is responsible for the glass transition, below which the system becomes a glass.

When a substance rapidly cooled into the temperature regime $T < T_g$, the physical properties of the material become time-dependent in this non-ergodic state, as the system attempts to reach equilibrium.[5,88,100–103] Time-dependent properties include: enthalpy, entropy, the compliance, gas permeability/selectivity, density, index of refraction, and dielectric susceptibility. In polymers, the physical aging process is characterized by three regimes: an initial plateau, an intermediate time-dependent stage, and an equilibrium plateau. The aging rate:[104]

$$\beta = \frac{1}{h_\infty}\frac{dh}{d\left[ln(t_{age})\right]}, \quad (5)$$

is obtained from the slope of the lines shown in Fig. 8(a).[33] The data shown in this figure represent the intermediate, time-dependent, aging stage. It is well established that the aging rate is determined by the difference between the glass-transition temperature of the material T_g and the aging temperature T_{age}: $T_g - T_{age} = \Delta T_a$.[100–103] For small values of ΔT_a the aging rate is fast and increases with increasing ΔT_a; however, the aging rate reaches a maximum and then decreases with increasing ΔT_a. This maximum is the result of two competing processes: the driving force for aging increases with decreasing ΔT_a, but the thermal energy decreases as T decreases. Experimentally, the time scale associated with achieving equilibrium could range from minutes to decades. In our case, we investigated the time dependent changes in the film thickness of a supported polymer film after it is quenched to a temperature T_{age}.

The aging rates of star-shaped and linear-chain polymers differ: whereas the aging rate of linear-chain polymers is independent of the length of the chain,[100–103] the rates of star-shaped polymers depend on the functionalities and on the arm lengths of the polymers.[32,33] It is shown in Fig. 9(a) that as the functionality of the star is increased the aging rate decreases at a constant temperature relative to T_g.[33] However, when M_{arm} is sufficiently large the star-shaped polymers exhibit an aging rate similar to linear-chain PS [Fig. 9(b)].[33] It should be intuitive, therefore, that as the length of the arms is increased, or the number of arms is decreased, the reduction of the aging rate associated with the branching point is suppressed.

It has been noted that the glass-transition temperature of a thin film is not a constant value, but varies as a function of distance from an interface. With regard to aging, the local aging rates of a film are dictated by the local T_gs throughout the depth of the film. This is illustrated in Figs. 10(a) and 10(b), where it is shown how the aging rate changes across thin films of linear-chain PS [Fig. 10(a)].[32] MD simulations of the aging of freely standing linear-chain polymer films yield similar results; the aging rate is lowest near the free surface and increases with increasing distance, reaching a maximum,

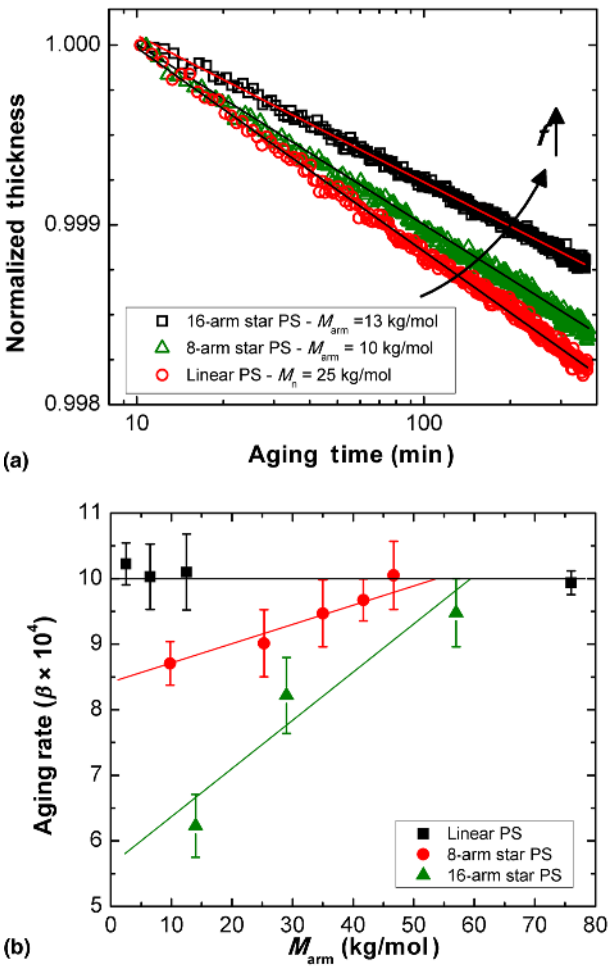

Figure 9. (a) The time-dependent change in film thickness for $h = 1000$ nm thick films of three different PSs: linear-chain and star-shaped ($f = 8$, 16). Reproduced (adapted) with permission from Ref. 33, copyright 2012 American Chemical Society. (b) The physical aging rate is plotted as a function of f and M_{arm} at a temperature which is 35 °C below the T_g for the $h = 1000$ nm thick films. The black squares represent linear PS, the red circles represent 8-arm star PS and green triangles represent 16 arm star PS. Reproduced (adapted) with permission from Ref. 33, copyright 2012 American Chemical Society.

in the interior of the film.[105] Note that in Fig. 10(a), the film is supported and T_g at the substrate is approximately equal to the bulk T_g for this linear-chain PS/SiO_x system, as discussed earlier. Hence, the aging rate necessarily reaches a plateau, as shown.[32] The aging rates for the 8-arm star-shaped PS [Fig. 10(b)] are also depth-dependent and also dependent on the difference between the aging temperature and the local T_g, i.e., the T_g at that depth.[32] The other important result of this model is shown in Fig. 9(c), which shows the lower T_g surface layer for the linear chain increases with increasing T, for temperatures below T_g. This is the liquid-like surface layer to which we referred in the section on the T_g of thin films; its thickness is dictated by $T_g - T$. These data in Fig. 10(c) are

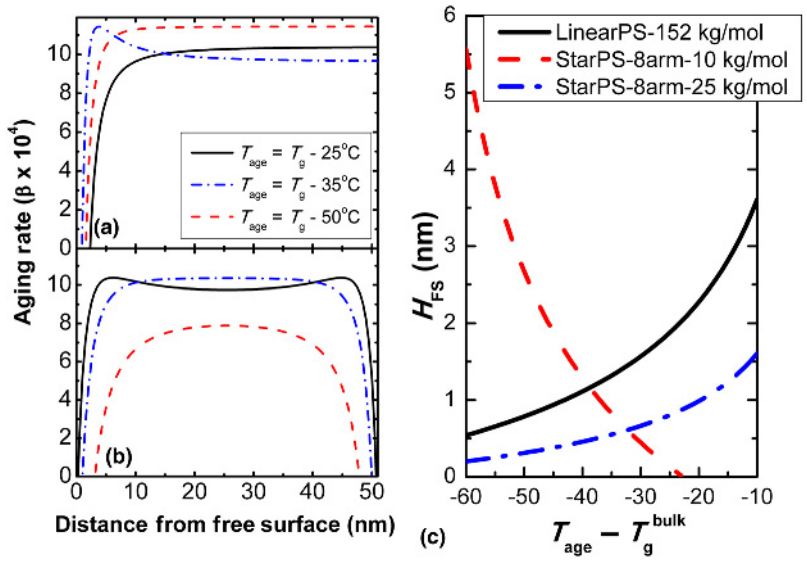

Figure 10. (a) The aging rate is shown here for linear-chain PS as a function of distance from the free surface, for a $h = 50$ nm thick film; (b) similar data are shown for the 8-arm star shaped PS. (c) The thicknesses of the surface layers are shown here at a function of the difference between the bulk T_g and the aging temperatures for linear-chain and star-shaped polymers. Reproduced (adapted) with permission from Ref. 32, copyright 2012 American Physical Society.

consistent, both in magnitude and the trend with temperature, with independent experiments by other researchers.[62,106] When the outer surface layer has a higher T_g than the bulk, the surface layer thickness decreases (opposite trend) over the same temperature range.

We conclude this section by reiterating the following observations. The aging of a thin film is dictated by the local T_gs near the interfaces. The average aging rates of star-shaped macromolecules are lower than that of their linear-chain analogs. This has important implications regarding the use of macromolecules of different architectures for thin-film membrane applications as well as a host of thin-film packaging applications.

Future outlook

Star-shaped polymers exhibit different physical properties from their linear-chain analogs when confined to thin-film geometries. The key differences include the following. (i) The surface wettability of star-shaped polymers may be "tailored" in a controllable manner by varying the functionality of a star-shaped polymer and the arm length. (ii) The substrate and free surface T_gs of the star-shaped polymers are dependent on the functionality and molecular mass per arm. (iii) Star-shaped polymers age more slowly than linear-chain polymers.

The practical implications of such differences are important for a variety of applications. The mechanical properties of films are sensitive to film thickness as shown by MD simulations,[107,108] finite-element analysis,[109] nanoindentation experiments,[110] thin-film buckling measurements,[13,111,112] and Brillouin light scattering. The thickness dependence is associated with the fact that near the free surface the local T_g is lower than the bulk T_g, which suppresses the average T_g of the film. The magnitude of the modulus depends on the difference between the bulk T_g and the ambient temperature at which the measurements are conducted. Star-shaped polymers would offer an important alternative to linear-chain polymers, because their interfacial properties are dictated by f and M_{arm}. Another obvious application would be adhesion to various types of interfaces, due to their enhanced wettability. Additionally, the star-shaped polymers may be suitable for membrane applications for gas selectivity and/or separation. Since the star-shaped macromolecules age at appreciably slower rates than the linear chains, they offer important advantages with regard to the stability and reliability of pore sizes in polymer membranes.

Acknowledgments

This publication is based on the work supported in part by the National Science Foundation (NSF), Division of Materials Research by award DMR-0906425 and award DMR-1305749. Certain commercial equipment, instruments, or materials are identified in this paper in order to specify the experimental procedure adequately. Such identification is not intended to imply recommendation or endorsement by the National Institute of Standards and Technology, nor is it intended to imply that the materials or equipment identified are necessarily the best available for the purpose.

References

1. J.L. Keddie, R.A.L. Jones, and R.A. Cory: Interface and surface effects on the glass-transition temperature in thin polymer films. *Faraday Discuss.* **98**, 219 (1994).

2. J.L. Keddie, R.A.L. Jones, and R.A. Cory: Size-dependent depression of the glass transition temperature in polymer films. *Europhys. Lett.* **27**, 59 (1994).
3. J.A. Forrest and K. Dalnoki-Veress: The glass transition in thin polymer films. *Adv. Colloid Interface Sci.* **94**, 167 (2001).
4. Z.H. Yang, Y. Fujii, F.K. Lee, C.H. Lam, and O.K.C. Tsui: Glass transition dynamics and surface layer mobility in unentangled polystyrene films. *Science* **328**, 1676 (2010).
5. R.D. Priestley, C.J. Ellison, L.J. Broadbelt, and J.M. Torkelson: Structural relaxation of polymer glasses at surfaces, interfaces and in between. *Science* **309**, 456 (2005).
6. M. Alcoutlabi and G.B. Mckenna: Effects of confinement on material behaviour at the nanometre size scale. *J. Phys.: Condens. Matter* **17**, R461 (2005).
7. T. Kanaya: Glass transition, dynamics and heterogeneity of polymer thin films preface, in *Glass Transition, Dynamics and Heterogeneity of Polymer Thin Films*, edited by T. Kanaya (Springer-Verlag Berlin, Berlin, 2013) pp. V.
8. J. Baschnagel and F. Varnik: Computer simulations of supercooled polymer melts in the bulk and in-confined geometry. *J. Phys.: Condens. Matter* **17**, R851 (2005).
9. J.E.G. Lipson and S.T. Milner: Percolation model of interfacial effects in polymeric glasses. *Eur. Phys. J. B* **72**, 133 (2009).
10. D. Long and F. Lequeux: Heterogeneous dynamics at the glass transition in van der Waals liquids, in the bulk and in thin films. *Eur. Phys. J. E* **4**, 371 (2001).
11. J.D. Mccoy and J.G. Curro: Conjectures on the glass transition of polymers in confined geometries. *J. Chem. Phys.* **116**, 9154 (2002).
12. J. Mittal, P. Shah, and T.M. Truskett: Using energy landscapes to predict the properties of thin films. *J. Phys. Chem. B* **108**, 19769 (2004).
13. C.M. Stafford, C. Harrison, K.L. Beers, A. Karim, E.J. Amis, M.R. Vanlandingham, H.C. Kim, W. Volksen, R.D. Miller, and E.E. Simonyi: A buckling-based metrology for measuring the elastic moduli of polymeric thin films. *Nat. Mater.* **3**, 545 (2004).
14. P.A. O'connell, S.A. Hutcheson, and G.B. Mckenna: Creep behavior of ultra-thin polymer films. *J. Polym. Sci. B: Polym. Phys.* **46**, 1952 (2008).
15. M.S. Mccaig and D.R. Paul: Effect of film thickness on the changes in gas permeability of a glassy polyarylate due to physical aging Part I. Experimental observations. *Polymer* **41**, 629 (2000).
16. M.S. Mccaig, D.R. Paul, and J.W. Barlow: Effect of film thickness on the changes in gas permeability of a glassy polyarylate due to physical aging Part II. Mathematical model. *Polymer* **41**, 639 (2000).
17. B.Y. Huang, E. Glynos, B. Frieberg, H.X. Yang, and P.F. Green: Effect of thickness-dependent microstructure on the out-of-plane hole mobility in poly(3-Hexylthiophene) films. *ACS Appl. Mater. Interfaces* **4**, 5204 (2012).
18. H.X. Yang, E. Glynos, B.Y. Huang, and P.F. Green: Out-of-plane carrier transport in conjugated polymer thin films: role of morphology. *J. Phys. Chem. C* **117**, 9590 (2013).
19. B.X. Dong, B.Y. Huang, A. Tan, and P.F. Green: Nanoscale orientation effects on carrier transport in a low-band-gap polymer. *J. Phys. Chem. C* **118**, 17490 (2014).
20. M. Bank, C. Thies, and J Leffingw: Thermally induced phase separation of polystyrene-poly(vinyl methyl-ether) mixtures. *J. Polym. Sci. B: Polym. Phys.* **10**, 1097 (1972).
21. M.M. Coleman, J.F. Graf, and P.C. Painter: *Specific Interactions and the Miscibility of Polymer Blends* (Technomic Publishing, Lancaster, PA, 1991).
22. M.M. Coleman and P.C. Painter: Hydrogen-bonded polymer blends. *Prog. Polym. Sci.* **20**, 1 (1995).
23. J. Dudowicz and K.F. Freed: Effect of monomer structure and compressibility on the properties of multicomponent polymer blends and solutions. 1. Lattice cluster theory of compressible systems. *Macromolecules* **24**, 5076 (1991).
24. J. Dudowicz and K.F. Freed: Effect of monomer structure and compressibility on the properties of multicomponent polymer blends and solutions3. Application to PS(D) PVME blends. *Macromolecules* **24**, 5112 (1991).
25. G. Coulon, T.P. Russell, V.R. Deline, and P.F. Green: Surface-induced orientation of symmetric, Diblock copolymers—a secondary ion mass-spectrometry study. *Macromolecules* **22**, 2581 (1989).
26. K.R. Shull: Mean-field theory of block copolymers—bulk melts, surfaces, and thin-films. *Macromolecules* **25**, 2122 (1992).
27. A. Menelle, T.P. Russell, S.H. Anastasiadis, S.K. Satija, and C. F. Majkrzak: Ordering of thin Diblock copolymer films. *Phys. Rev. Lett.* **68**, 67 (1992).
28. E. Glynos, A. Chremos, B. Frieberg, G. Sakellariou, and P.F. Green: Wetting of macromolecules: from linear chain to soft colloid-like behavior. *Macromolecules* **47**, 1137 (2014).
29. E. Glynos, B. Frieberg, and P.F. Green: Wetting of a multiarm star-shaped molecule. *Phys. Rev. Lett.* **107**, 118303 (2011).
30. E. Glynos, B. Frieberg, H. Oh, M. Liu, D.W. Gidley, and P.F. Green: Role of molecular architecture on the vitrification of polymer thin films. *Phys. Rev. Lett.* **106**, 128301 (2011).
31. E. Glynos, B. Frieberg, A. Chremos, G. Sakellariou, D.W. Gidley, and P. F. Green: Vitrification of thin polymer films: from linear chain to soft colloid-like behavior. *Macromolecules* **48**, 2305 (2015).
32. B. Frieberg, E. Glynos, and P.F. Green: Structural relaxations of thin polymer films. *Phys. Rev. Lett.* **108**, 268304 (2012).
33. B. Frieberg, E. Glynos, G. Sakellariou, and P.F. Green: Physical aging of star-shaped macromolecules. *ACS Macro Lett.* **1**, 636 (2012).
34. S.F. Wang, Z. Jiang, S. Narayanan, and M.D. Foster: Dynamics of surface fluctuations on macrocyclic melts. *Macromolecules* **45**, 6210 (2012).
35. S.F. Wang, S. Yang, J. Lee, B. Akgun, D.T. Wu, and M.D. Foster: Anomalous surface relaxations of branched-polymer melts. *Phys. Rev. Lett.* **111**, 068303 (2013).
36. D. Vlassopoulos and G. Fytas: From polymers to colloids: engineering the dynamic properties of hairy particles, in *High Solid Dispersions*, edited by M. Cloitre (Springer-Verlag, Berlin, 2010), pp. 1.
37. A. Chremos, E. Glynos, and P.F. Green: Structure and dynamical intramolecular heterogeneity of star polymer melts above glass transition temperature. *J. Chem. Phys.* **142**, 044901 (2015).
38. D.S. Pearson and E. Helfand: Viscoelastic properties of star-shaped polymers. *Macromolecules* **17**, 888 (1984).
39. P.G. Degennes and P. Pincus: scaling theory of polymer adsorption—proximal exponent. *J. Phys. Lett.* **44**, L241 (1983).
40. M. Rubinstein and R.H. Colby: *Polymer Physics* (Oxford University Press, New York, 2003).
41. D.Y. Yoon, M. Vacatello, and G.D. Smith: *Monte Carlo and Molecular Dynamics Simulations in Polymer Science* (Oxford University Press, New York, 1995).
42. T.K. Xia, O.Y. Jian, M.W. Ribarsky, and U. Landman: Interfacial alkane films. *Phys. Rev. Lett.* **69**, 1967 (1992).
43. O. Borodin, G.D. Smith, R. Bandyopadhyaya, and E. Byutner: Molecular dynamics study of the influence of solid interfaces on poly(ethylene oxide) structure and dynamics. *Macromolecules* **36**, 7873 (2003).
44. K.C. Daoulas, V.A. Harmandaris, and V.G. Mavrantzas: Detailed atomistic simulation of a polymer melt/solid interface: structure, density, and conformation of a thin film of polyethylene melt adsorbed on graphite. *Macromolecules* **38**, 5780 (2005).
45. D.N. Theodorou: Variable-density model of polymer melt solid interfaces—structure, adhesion tension, and surface forces. *Macromolecules* **22**, 4589 (1989).
46. K.F. Mansfield and D.N. Theodorou: Molecular-dynamics simulation of a glassy polymer surface. *Macromolecules* **24**, 6283 (1991).
47. D.M. Sussman, W.-S. Tung, K.I. Winey, K.S. Schweizer, and R. A. Riggleman: Entanglement Reduction and anisotropic chain and primitive path conformations in polymer melts under thin film and cylindrical confinement. *Macromolecules* **47**, 6462 (2014).
48. C.H. Ye, C.G. Wiener, M. Tyagi, D. Uhrig, S.V. Orski, C.L. Soles, B.D. Vogt, and D.S. Simmons: Understanding the decreased segmental dynamics of supported thin polymer films reported by incoherent neutron scattering. *Macromolecules* **48**, 801 (2015).
49. C. Soles, J. Douglas, W.L. Wu, and R. Dimeo: Incoherent neutron scattering and the dynamics of confined polycarbonate films. *Phys. Rev. Lett.* **88**, 037401 (2002).
50. C.L. Soles, J.F. Douglas, and W.-L. Wu: Dynamics of thin polymer films: recent insights from incoherent neutron scattering. *J. Polym. Sci. B: Polym. Phys.* **42**, 3218 (2004).

51. S. Napolitano, S. Capponi, and B. Vanroy: Glassy dynamics of soft matter under 1D confinement: how irreversible adsorption affects molecular packing, mobility gradients and orientational polarization in thin films. *Eur. Phys. J. E* **36**, 61 (2013).
52. S. Napolitano and M. Wubbenhorst: The lifetime of the deviations from bulk behaviour in polymers confined at the nanoscale. *Nat. Commun.* **2**, 260 (2011).
53. C.L. Soles, J.F. Douglas, W.L. Wu, H.G. Peng, and D.W. Gidley: Comparative specular x-ray reflectivity, positron annihilation lifetime spectroscopy, and incoherent neutron scattering measurements of the dynamics in thin polycarbonate films. *Macromolecules* **37**, 2890 (2004).
54. L. Yelash, P. Virnau, K. Binder, and W. Paul: Three-step decay of time correlations at polymer-solid interfaces. *Eerophys. Lett.* **98**, 5 (2012).
55. S. Peter, H. Meyer, and J. Baschnagel: Molecular dynamics simulations of concentrated polymer solutions in thin film geometry. I. Equilibrium properties near the glass transition. *J. Chem. Phys.* **131**, 7 (2009).
56. P.Z. Hanakata, J.F. Douglas, and F.W. Starr: Interfacial mobility scale determines the scale of collective motion and relaxation rate in polymer films. *Nat. Commun.* **5**, 8 (2014).
57. Y. Chai, T. Salez, J.D. Mcgraw, M. Benzaquen, K. Dalnoki-Veress, E. Raphaël, and J.A. Forrest: A direct quantitative measure of surface mobility in a glassy polymer. *Science* **343**, 994 (2014).
58. P.G. De Gennes: Glass transitions in thin polymer films. *Eur. Phys. J. E* **2**, 201 (2000).
59. M.D. Ediger and J.A. Forrest: Dynamics near free surfaces and the glass transition in thin polymer films: a view to the future. *Macromolecules* **47**, 471 (2013).
60. C.J. Ellison and J.M. Torkelson: The distribution of glass-transition temperatures in nanoscopically confined glass formers. *Nat. Mater.* **2**, 695 (2003).
61. Z. Fakhraai and J.A. Forrest: Measuring the surface dynamics of glassy polymers. *Science* **319**, 600 (2008).
62. K. Paeng, S.F. Swallen, and M.D. Ediger: Direct measurement of molecular motion in freestanding polystyrene thin films. *J. Am. Chem. Soc.* **133**, 8444 (2011).
63. J.E. Pye and C.B. Roth: Two simultaneous mechanisms causing glass transition temperature reductions in high molecular weight freestanding polymer films as measured by transmission ellipsometry. *Phys. Rev. Lett.* **107**, 5 (2011).
64. J.A. Torres, P.F. Nealey, and J.J. De Pablo: Molecular simulation of ultrathin polymeric films near the glass transition. *Phys. Rev. Lett.* **85**, 3221 (2000).
65. F. Lange, P. Judeinstein, C. Franz, B. Hartmann-Azanza, S. Ok, M. Steinhart, and K. Saalwächter: Large-scale diffusion of entangled polymers along nanochannels. *ACS Macro Lett.* **4**, 561 (2015).
66. D. Bonn, J. Eggers, J. Indekeu, J. Meunier, and E. Rolley: Wetting and spreading. *Rev. Mod. Phys.* **81**, 739 (2009).
67. P.G. De Gennes, F. Brochard-Wyart, and D. Quere: *Capillarity and Wetting Phenomena* (Springer-Verlag, New York, Inc., New York, 2004).
68. P.G. Degennes: Wetting—statics and dynamics. *Rev. Mod. Phys.* **57**, 827 (1985).
69. L. Leger and J.F. Joanny: Liquid spreading. *Rep. Prog. Phys.* **55**, 431 (1992).
70. T. Young: An essay on the cohesion of fluids. *Philos. Trans. R. Soc. Lond.* **95**, 65 (1805).
71. A. Striolo and J.M. Prausnitz: Adsorption of branched homopolymers on a solid surface. *J. Chem. Phys.* **114**, 8565 (2001).
72. V.S. Minnikanti and L.A. Archer: Entropic attraction of polymers toward surfaces and its relationship to surface tension. *Macromolecules* **39**, 7718 (2006).
73. Z.Y. Qian, V.S. Minnikanti, B.B. Sauer, G.T. Dee, and L.A. Archer: Surface tension of symmetric star polymer melts. *Macromolecules* **41**, 5007 (2008).
74. M.K. Kosmas: Ideal polymer-chains of various architectures at a surface. *Macromolecules* **23**, 2061 (1990).
75. A. Chremos, P.J. Camp, E. Glynos, and V. Koutsos: Adsorption of star polymers: computer simulations. *Soft Matter* **6**, 1483 (2010).
76. J.A. Forrest, K. Dalnokiveress, and J.R. Dutcher: Interface and chain confinement effects on the glass transition temperature of thin polymer films. *Phys. Rev. E* **56**, 5705 (1997).
77. J.A. Forrest, K. Dalnokiveress, J.R. Stevens, and J.R. Dutcher: Effect of free surfaces on the glass transition temperature of thin polymer films. *Phys. Rev. Lett.* **77**, 2002 (1996).
78. J.A. Forrest and J. Mattsson: Reductions of the glass transition temperature in thin polymer films: Probing the length scale of cooperative dynamics. *Phys. Rev. E* **61**, R53 (2000).
79. M.D. Ediger and J.A. Forrest: Dynamics near free surfaces and the glass transition in thin polymer films: a view to the future. *Macromolecules* **47**, 471 (2014).
80. S. Kawana and R.a.L. Jones: Character of the glass transition in thin supported polymer films. *Phys. Rev. E* **63**, 021401 (2001).
81. R. Priestley, M.K. Mundra, N.J. Barnett, L.J. Broadbelt, and J.M. Torkelson: Effects of nanoscale confinement and interfaces on the glass transition temperatures of a series of poly(n-methacrylate) films. *Aust. J. Chem.* **60**, 765 (2007).
82. J.H. Kim, J. Jang, and W.C. Zin: Thickness dependence of the glass transition temperature in thin polymer films. *Langmuir* **17**, 2703 (2001).
83. J.Q. Pham and P.F. Green: The glass transition of thin film polymer/polymer blends: interfacial interactions and confinement. *J. Chem. Phys.* **116**, 5801 (2002).
84. J.Q. Pham and P.F. Green: Effective T-g of confined polymer–polymer mixtures. Influence of molecular size. *Macromolecules* **36**, 1665 (2003).
85. J.A. Forrest: What can we learn about a dynamical length scale in glasses from measurements of surface mobility? *J. Chem. Phys.* **139**, 084702 (2013).
86. A. Shavit and R.A. Riggleman: Influence of backbone rigidity on nanoscale confinement effects in model glass-forming polymers. *Macromolecules* **46**, 5044 (2013).
87. S. Mirigian and K.S. Schweizer: Communication: slow relaxation, spatial mobility gradients, and vitrification in confined films. *J. Chem. Phys.* **141**, 5 (2014).
88. L.C.E. Struik: *Physical Aging in Amorphous Polymers* (Elsevier Scientific Publishing Company, Amsterdam, 1978).
89. J. Zhao, S.L. Simon, and G.B. Mckenna: Using 20-million-year-old amber to test the super-Arrhenius behaviour of glass-forming systems. *Nat. Commun.* **4**, 6 (2013).
90. J.P. Bouchaud: Weak ergodicity breaking and aging in disordered-systems. *J. Phys. I* **2**, 1705 (1992).
91. W.H. Wang: The elastic properties, elastic models and elastic perspectives of metallic glasses. *Prog. Mater. Sci.* **57**, 487 (2012).
92. G.S. Fulcher: Analysis of recent measurements of the viscosity of glasses. *J. Am. Ceram. Soc.* **8**, 339 (1925).
93. G. Tammann and W. Hesse: The dependency of viscosity on temperature in hypothermic liquids. *Z. Anorg. Allg. Chem.* **156**, 245 (1926).
94. H. Vogel: The temperature dependence law of the viscosity of fluids. *Phys. Z.* **22**, 645 (1921).
95. M.L. Williams, R.F. Landel, and J.D. Ferry: Mechanical properties of substances of high molecular weight 19. the temperature dependence of relaxation mechanisms in amorphous polymers and other glass-forming liquids. *J. Am. Chem. Soc.* **77**, 3701 (1955).
96. G. Adam and J.H. Gibbs: On temperature dependence of cooperative relaxation properties in glass-forming liquids. *J. Chem. Phys.* **43**, 139 (1965).
97. M.D. Ediger: Spatially heterogeneous dynamics in supercooled liquids. *Annu. Rev. Phys. Chem.* **51**, 99 (2000).
98. L. Berthier and G. Biroli: Theoretical perspective on the glass transition and amorphous materials. *Rev. Mod. Phys.* **83**, 587 (2011).
99. F.W. Starr, J.F. Douglas, and S. Sastry: The relationship of dynamical heterogeneity to the Adam–Gibbs and random first-order transition theories of glass formation. *J. Chem. Phys.* **138**, 12A541 (2013).
100. J.M. Hutchinson: Physical aging of polymers. *Prog. Polym. Sci.* **20**, 703 (1995).
101. A.J. Kovacs, J.J. Aklonis, J.M. Hutchinson, and A.R. Ramos: Isobaric volume and enthalpy recovery of glasses .2. Transparent multiparameter theory. *J. Polym. Sci. B: Polym. Phys.* **17**, 1097 (1979).
102. I.M. Hodge: Physical aging in polymer glasses. *Science* **267**, 1945 (1995).

103. G.B. Mckenna: Mechanical rejuvenation in polymer glasses: fact or fallacy? *J. Phys.: Condens. Matter* **15**, S737 (2003).
104. E.A. Baker, P. Rittigstein, J.M. Torkelson, and C.B. Roth: Streamlined ellipsometry procedure for characterizing physical aging rates of thin polymer films. *J. Polym. Sci. B: Polym. Phys.* **47**, 2509 (2009).
105. A. Shavit and R.A. Riggleman: Physical aging, the local dynamics of glass-forming polymers under nanoscale confinement. *J. Phys. Chem. B* **118**, 9096 (2014).
106. K. Paeng and M.D. Ediger: Molecular motion in free-standing thin films of poly(methyl methacrylate), poly(4-tert-butylstyrene), poly(alpha-methylstyrene), and poly(2-vinylpyridine). *Macromolecules* **44**, 7034 (2011).
107. T.R. Bohme and J.J. De Pablo: Evidence for size-dependent mechanical properties from simulations of nanoscopic polymeric structures. *J. Chem. Phys.* **116**, 9939 (2002).
108. K. Yoshimoto, T.S. Jain, P.F. Nealey, and J.J. De Pablo: Local dynamic mechanical properties in model free-standing polymer thin films. *J. Chem. Phys.* **122**, 144712 (2005).
109. C.A. Clifford and M.P. Seah: Modelling of nanomechanical nanoindentation measurements using an AFM or nanoindenter for compliant layers on stiffer substrates. *Nanotechnology* **17**, 5283 (2006).
110. C.A. Clifford and M.P. Seah: Nanoindentation measurement of Young's modulus for compliant layers on stiffer substrates including the effect of Poisson's ratios. *Nanotechnology* **20**, 145708 (2009).
111. C.M. Stafford, B.D. Vogt, C. Harrison, D. Julthongpiput, and R. Huang: Elastic moduli of ultrathin amorphous polymer films. *Macromolecules* **39**, 5095 (2006).
112. J.M. Torres, C.M. Stafford, and B.D. Vogt: Elastic modulus of amorphous polymer thin films: relationship to the glass transition temperature. *ACS Nano* **3**, 2677 (2009).